JOURNAL OF MATERIALS SCIENCE 29 (1994) 6069–6075

Silicon–aluminium network composites fabricated by liquid metal infiltration

YUYONG CHEN, D. D. L. CHUNG
Composite Materials Research Laboratory, State University of New York at Buffalo, Box 604400, Buffalo, NY 14260-4400, USA

This paper provides a new method for fabricating interpenetrating silicon–aluminium network metal-matrix composites. This method involves the infiltration of an aluminium–silicon alloy (Al–12Si–1Mg or Al–30Si–1Mg) liquid into a silicon particle (50 vol%) preform. The silicon particles were partially dissolved by the liquid alloy and, together with silicon contributed by the original Al–Si–Mg matrix, resulted in an Si network after solidification. The network composites were metallurgically sound, with no porosity, and exhibited a thermal expansion coefficient down to $7.7 \times 10^{-6}\,^{\circ}C^{-1}$ at 50–100 °C, compressive strength up to 580 MPa, tensile strength up to 160 MPa and Vickers hardness up to 390.

1. Introduction

Low-thermal-expansion thermal conductors are important for use as heat sinks, back planes, substrates and housings in electronic packages. The requirement for these components to have low thermal expansion originates from the low thermal expansion of the semiconductor (e.g. silicon gallium arsenide) and the need for the electronic package to withstand thermal cycling. In the case of aerospace electronics, a low density is also desired. Aerospace structure materials have similar requirements, except that they further require high strength and high modulus. As the thermal expansion coefficients (CTEs) of silicon and gallium arsenide are 4.2×10^{-6} and $6.5 \times 10^{-6}\,^{\circ}C^{-1}$, respectively, at 25 °C, the CTEs of the electronic packaging material should approach these values, which are very low compared to those of metals such as aluminium (CTE = $23.6 \times 10^{-6}\,^{\circ}C^{-1}$). In spite of its high CTE, aluminium is attractive in its low density, good processability and low cost.

The most effective way of decreasing the CTE of aluminium is the addition of a low-CTE filler, which can be in the form of particles, whiskers of fibres, to form an aluminium-matrix composite. For large reduction of the CTE, the volume fraction of the filler must be high. In general, using particles as the filler can lead to a higher volume fraction than with whiskers or short fibres as the filler. Nevertheless, the amount of the matrix aluminium must be sufficient to hold the particles together. In the case of the composites fabricated by liquid metal infiltration, the filler volume fraction must be low enough so that there are sufficient channels in the preform for the liquid metal to go through.

In order to obtain a low-CTE composite, the filler volume fraction should be high while the filler–matrix interface area is large and soundness is maintained in the composite. A composite in which (i) the filler volume fraction is high and (ii) the low-CTE filler and the high-CTE metal are both continuous, such that they are in the form of interpenetrating networks with a fine microstructure, is thus expected to be attractive. In this work we have indeed made such a composite, where the low-CTE filler volume fraction was up to 69% and the low-CTE filler network's microstructure feature size was 2–5 μm.

A large variety of particulate fillers have been used to produce low thermal expansion aluminium-matrix composites. They include SiC, Al_2O_3, AlN and Si. Due to the additional desire for a high thermal conductivity in the composite, a filler with a relatively high thermal conductivity is preferred. Thus SiC, AlN and Si are preferred to Al_2O_3. Silicon has a low CTE and a high bulk modulus (primarily due to its unusually high Poisson's ratio) [1]. In the case of Si as the filler, a particulate (not network) composite made by powder metallurgy and consisting of 60 wt % Al and 40 wt% Si is commercially available from Sumitomo Electric Industries, Japan (CMSH A-40). This composite exhibits a CTE of $13.0 \times 10^{-6}\,^{\circ}C^{-1}$ at 25 °C and $15.4 \times 10^{-6}\,^{\circ}C^{-1}$ at 400 °C, and a thermal conductivity of 126 $Wm^{-1}K^{-1}$ at 25 °C [2]. In contrast, for plain aluminium the CTE is $23.6 \times 10^{-6}\,^{\circ}C^{-1}$ and the thermal conductivity is 247 $Wm^{-1}K^{-1}$ [3]. The fabrication of Si–Al composites by liquid Al infiltration rather than powder metallurgy is complicated by the tendency for liquid Al to dissolve the Si particles. The Al–Si alloy liquid formed pushes the Si particles as infiltration occurs, thereby causing channelling and related non-uniformity in the resulting composite. This problem diminishes as the Si content in the aluminium matrix increases.

The fabrication of the new interpenetrating network composite requires a novel composite fabrication technique that involves liquid metal alloy infiltration into a filler particulate preform, such that (i) the liquid alloy contains the filler as an alloying element, (ii) the liquid alloy partly dissolves the filler particles, and (iii)

0022-2461

the liquid alloy contributes to the eventual filler network. That the liquid alloy contains the filler as an alloying element is needed in order to reach a high filler volume fraction. That the liquid alloy partly dissolves the filler particles and contributes to the filler network is needed in order to form a filler network. In this work, the filler was silicon and the alloy used was either Al–12Si–1Mg or Al–30Si–1Mg. The filler network was not present prior to infiltration; rather it was formed during infiltration and subsequent solidification. The preform used was silicon particles occupying 50 vol% of the preform volume and held by a small proportion (~ 0.1 wt %) of an acid phosphate binder. The resulting silicon network constituted up to 69% of the volume of the composite. The aluminium was introduced by infiltration, so it necessarily formed a network too, though the aluminium network only constitutes the minor part of the composite. In order to obtain a fine feature size for the low-CTE filler network, the particles used in this preform must be sufficiently fine. In this work the Si particles used were of size 1–5 μm, thus resulting in a network feature size about 2–5 μm.

2. Experimental procedure

2.1. Composite fabrication

The alloys used were the eutectic alloy Al–12Si–1 Mg and the hypereutectic alloy Al–30Si–1Mg, the liquidus temperatures of which were 577 and 820 °C, respectively. The magnesium in the alloys served to enhance the wetting of the silicon particulate preform by the liquid alloys. Fig. 1a shows the microstructure of the eutectic Al–12Si–1Mg alloy; it consists of an α-Al dendrite structure and the eutectic silicon phase. Fig. 1b shows the microstructure of the hypereutectic Al–30Si–1Mg alloy; the primary silicon appeared as particles of size about 200 μm. The CTEs of the eutectic and hypereutectic alloys were 19.62×10^{-6} and 16.86×10^{-6} °C, respectively, at 50–100 °C (Table I).

The filler particles were 99.99 wt % Si (at least partly crystalline), as provided by KamaNord Industrikemi (Sicomill E). The particle size was 1–5 μm (Fig. 2).

The silicon particle preform was formed by wet-forming an Si–H_2O slurry containing a small amount of an acid phosphate binder [4]. The wet-forming was performed by cold-pressing at 5 MPa. After that, the preform was removed from the mould and dried at 200 °C for 24 h. After drying, the preform was heated in air at 400 °C for 4 h. It contained 50 vol %Si.

The composites were made by vacuum infiltration of the liquid metal under an argon pressure of 6000 p.s.i. (41 MPa) and an infiltration temperature of 800 °C for the eutectic Al–12Si–1Mg alloy and 900 °C for the hypereutectic Al–30Si–1Mg alloy. A steel mould was used. The process is similar to that described previously [5].

2.2. Composite characterization

Microstructural characterization of the composites included optical metallography and scanning electron microscopy (SEM). Metallographic samples were sectioned with a low-speed diamond saw, ground and then polished with a diamond paste. Etching was performed to remove a part of the aluminium in the composites. Light etching was performed by immersion in a 0.5 wt % HF water solution at room temperature for 3 min; heavy etching was performed by immersion in a 10 wt % NaOH water solution at 100 °C for 1 h. Elemental analysis was performed with

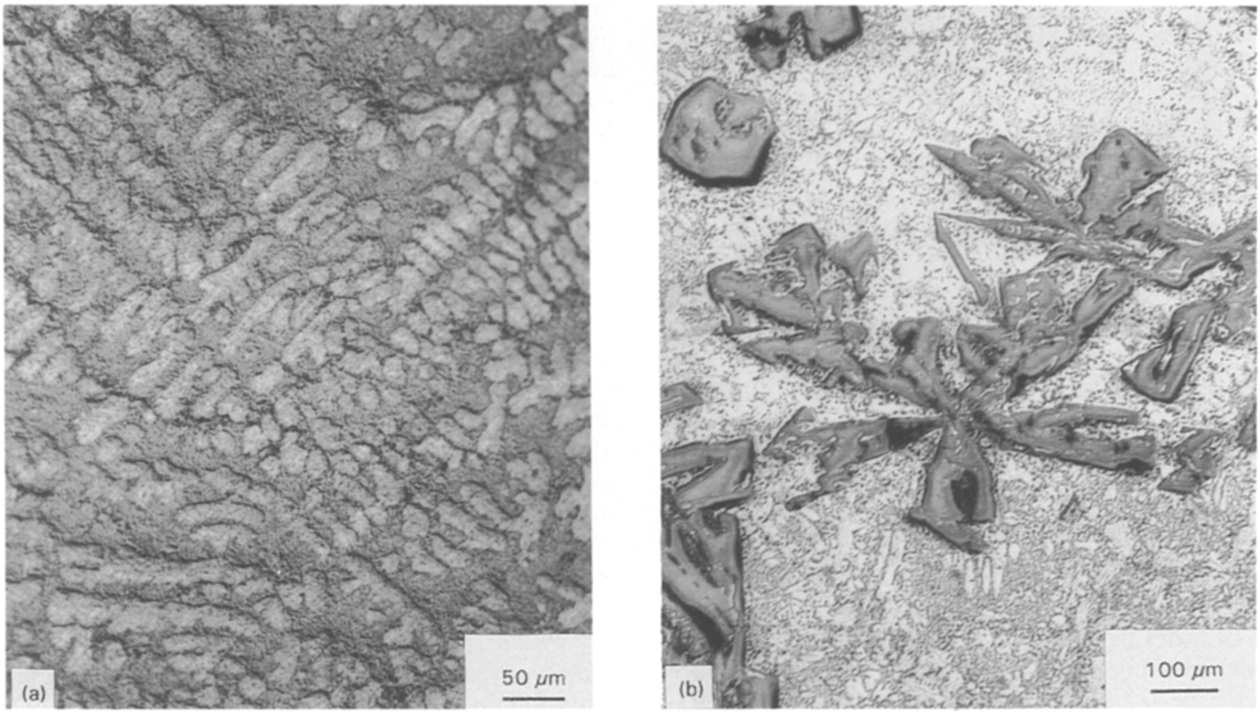

Figure 1 Optical micrographs of Al–Si–Mg alloys: (a) Al–12Si–1Mg, (b) Al–30Si–1Mg.

TABLE I CTE of Al–Si/Si composites

	CTE (10^{-6} °C^{-1})		
Alloy	50–100 °C	50–200 °C	50–300 °C
Al–12Si	19.62	19.78	20.34
Al–30Si	16.86	17.21	17.89
Al–40Si[a]	13.80	14.30	14.80
Al–12Si/Si	10.72	11.20	11.50
Al–30Si/Si	7.69	8.05	8.35

[a] Sumitomo.

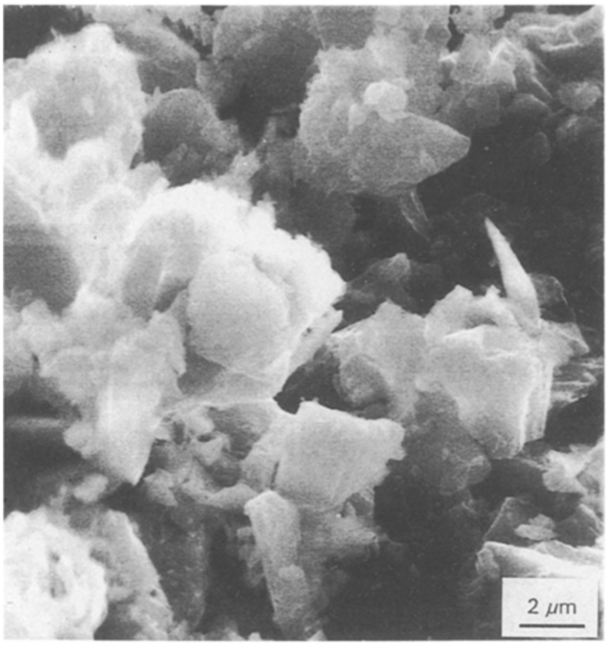

Figure 2 SEM micrographs of Si particle cluster (without any binder).

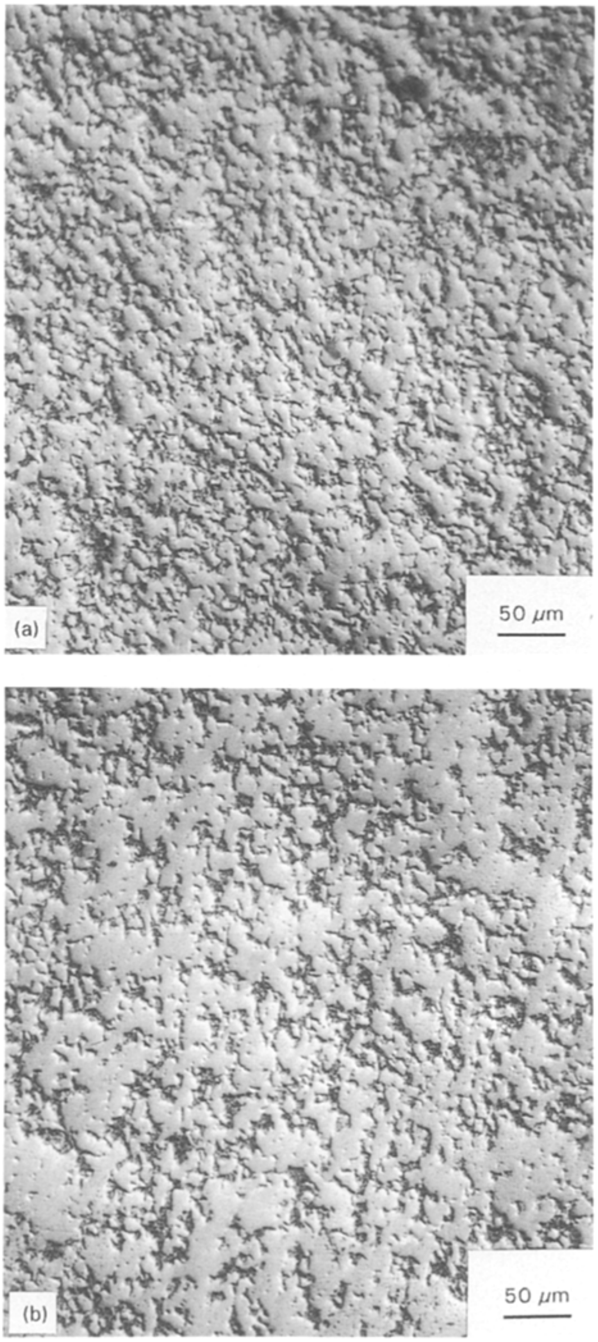

Figure 3 Optical micrographs of the Al–Si–Mg/Si composites: (a) Al–12Si–1Mg/Si, (b) Al–30Si–1Mg/Si.

energy-dispersive X-ray spectroscopy (EDS). The CTEs of the composites were measured by using a thermal mechanical analyser (Perkin–Elmer TMA7) operated at a heating rate of 5 °C min^{-1}. The Vickers microhardness (H_V), tensile strength, compressive strength and scratch resistance of the composites were measured. The scratch test was performed with a Teledyne Taber model 139 scratch tester, equipped with a Taber S-20 contour tungsten carbide shear tool. The applied load on the tool was 1000 g. The uniform scratch (groove) was used for determination of the scratch width with the help of a 10 × magnifier. The larger was the scratch width, the lower was the shear strength.

3. Results and discussion

Typical microstructures of the Al–Si–Mg/Si composites with the two different alloy matrices, as shown by optical microscopy, are depicted in Fig. 3. In both composites the silicon was in the form of a network, which was quite uniform. The network is more clear in Fig. 4, which shows SEM micrographs of the Al–30Si–1Mg/Si composite after a part of the aluminium in the composite had been removed by etching.

For the composite with Al–12Si–1Mg as the matrix, the silicon network constituted 57 vol % of the composite while the aluminium network constituted 43 vol %; X-ray spectroscopy showed that the silicon network contained about 97 wt %Si (Fig. 5, point 2), while the aluminium network contained about 3 wt % Si (Fig. 5, point 1). For the composite with Al–30Si–1Mg as the matrix, the silicon network constituted 69 vol % of the composite while the aluminium network constituted 31 vol %; X-ray spectroscopy showed that the silicon network contained about 96 wt% Si (Fig. 6, point 2), while the aluminium network contained about 8 wt % Si (Fig. 6, point 1). The feature size of the silicon network for both Al–12Si–1Mg/Si and Al–30Si–1Mg/Si composites was about 2–5 μm. The Si particles originally in the

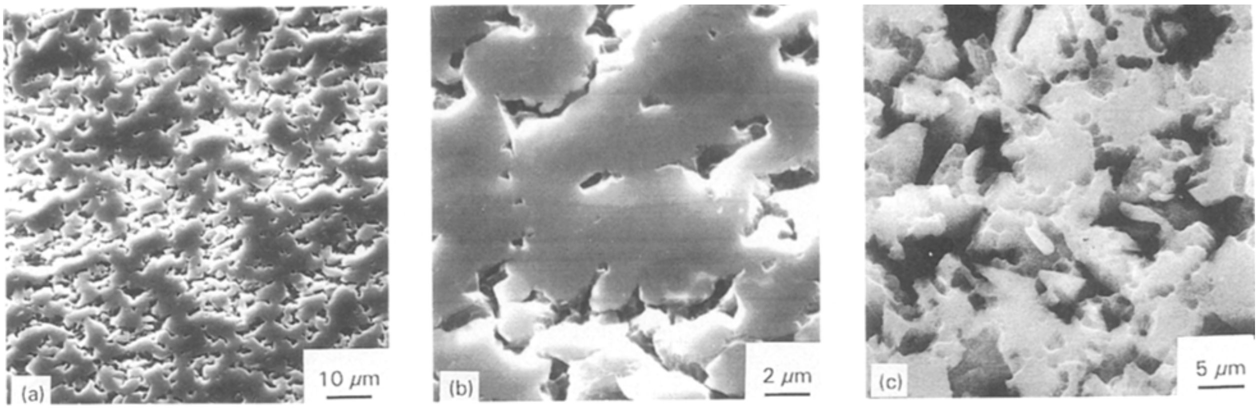

Figure 4 SEM micrographs of Al–30Si–1Mg/Si composite after (a, b) light etching and (c) heavy etching.

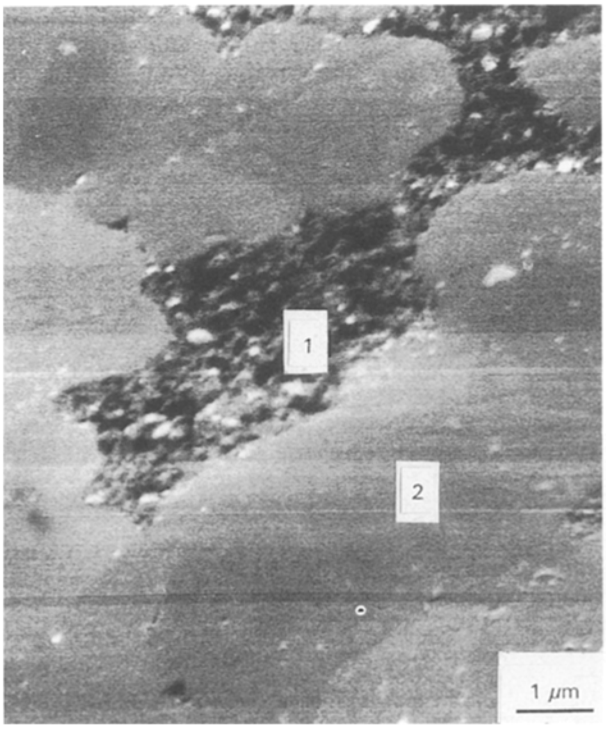

Figure 5 SEM micrographs of Al–12Si–1Mg/Si composite: (1) aluminium network, (2) silicon network.

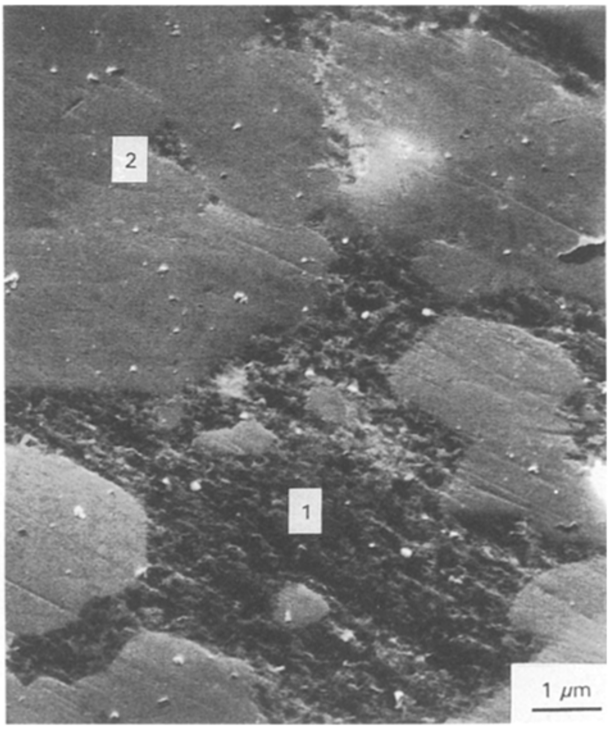

Figure 6 SEM micrographs of Al–30Si–1Mg/Si composite: (1) aluminium network, (2) silicon network.

preform could no longer be discerned. The volume fraction of the silicon network increased as the silicon content in the Al–Si matrix increased.

The microstructure of the composites was uniform, in contrast to the relative non-uniformity (dark patches) in a particulate (not network) composite made by Sumitomo (CMSH A-40) by powder metallurgy and consisting of 60 wt % Al and 40 wt % Si (Fig. 7).

During the composite fabrication by pressure casting, excess alloy was cast around the preform. The large silicon microstructural feature size in the excess alloy (lower parts of Fig. 8a and b and the whole of Fig. 8c) is related to the primary silicon there. The microstructure was much finer in the composite (upper parts of Fig. 8a and b) than in the excess alloy.

For the composite with Al–12Si–1Mg as the matrix, such that the Si network contained 97 wt % Si and the Al network contained 3 wt % Si, the known Si content of the overall composite requires that the volume fraction of the Si network be 57%, which is the same as the experimental value of 57 vol %. For the composite with Al–30Si–1Mg as the matrix, such that the Si network contained 96 wt % Si and the Al network contained 8 wt % Si, the known Si content of the overall composite requires that the volume fraction of the Si network be 66%, which is close to the experimental value of 69 vol %.

If all the silicon in the Al–12Si–1Mg matrix contributed to the filler network, the filler network would amount to 57 vol % of the composite. The observed network volume fraction of 57% is the same as the calculated value of 57%, indicating that the silicon in the Al–12Si–1Mg matrix contributed to the network formation. If all the silicon in the Al–30Si–1Mg matrix contributed to the filler network, the filler network

Figure 7 Optical micrographs of the Al–40Si composite (Sumitomo).

would amount to 67 vol % of the composite. The observed network volume fraction of 69% is quite close to the calculated value of 67%, indicating that the silicon in the Al–30Si–1Mg matrix also contributed to the network formation.

The solubility of Si in the Al–Si melt is 12 wt % Si at 577 °C, 28 wt % Si at 800 °C, 30 wt % Si at 820 °C and 37 wt % Si at 900 °C, according to the Al–Si phase diagram. At the infiltration temperature of 800 °C for the Al–12Si–1Mg melt, or 900 °C for the Al–30Si–1Mg melt, additional Si could be dissolved in the melt. A simple calculation shows that 25% of the Si particles were dissolved by the Al–12Si–1Mg melt at 800 °C, and 12% of Si particles were dissolved by the Al–30Si–1Mg melt at 900 °C.

The network formation was made possible by (i) the dissolution of a part of the Si particles and (ii) the contribution of silicon (about 69 − 50 = 19 vol % of the Al–30Si–1Mg matrix composite and about 57–50 = 7 vol % of the Al–12Si–1Mg matrix composite) from the original Al–Si matrix to the network. The original Si particles and the original primary silicon could not be discerned in the resulting silicon network.

The CTE values of the Al–12Si–1Mg/Si and Al–30Si–1Mg/Si composites were lower than that of Sumitomo's Al/Si (40 wt % Si) composite (Table I). The CTE decreased as the silicon content in the Al–Si matrix increased. The CTE values calculated by using the rule of mixtures were $12.21 \times 10^{-6}\,^{\circ}\mathrm{C}^{-1}$ for the Al–12Si–1Mg/Si composite and $10.20 \times 10^{-6}\,^{\circ}\mathrm{C}^{-1}$ for the Al–30Si–1Mg/Si composite. The measured values were lower than the calculated ones. The low CTE (as low as of $7.69 \times 10^{-6}\,^{\circ}\mathrm{C}^{-1}$) for the new composites of this work is comparable to those of conventional aluminium-matrix composites containing more than 70 vol % particles (SiC, AlN etc.) [6, 7].

The microhardness of the Al–Si/Si composites increased significantly as the volume fraction of silicon increased. The microhardness values (H_V) of Al–12Si–1Mg/Si and Al–30Si–1Mg/Si were 330 and 386, respectively, as compared to a value of only 150 for Sumitomo's Al/Si (40 wt % Si) composite (Table II).

The compressive strength of the Al–Si/Si composites increased as the silicon content increased. The compressive strengths of Al–12Si–1Mg/Si and Al–30Si–1Mg/Si were 525.7 and 584.1 MPa, respectively (Table III). However, the tensile strength of the Al–Si/Si composites was lower than that of Sumitomo's Al/Si (40 wt % Si) composite (Table IV). There are two reasons for this difference in tensile strength: (i) the composites of this work had a higher silicon content than that of Sumitomo, and (ii) the cooling rate in the liquid metal infiltration process of this work was low. Moreover, the tensile strength of the Al–30Si cast alloy was lower than that of Sumitomo's Al–40Si material, because the Sumitomo material was made by rapid solidification. In addition, the tensile strength of the Al–12Si cast alloy was higher than that of the Al–30Si cast alloy, because of the finer microstructure of Al–12Si (Fig. 1). As a result

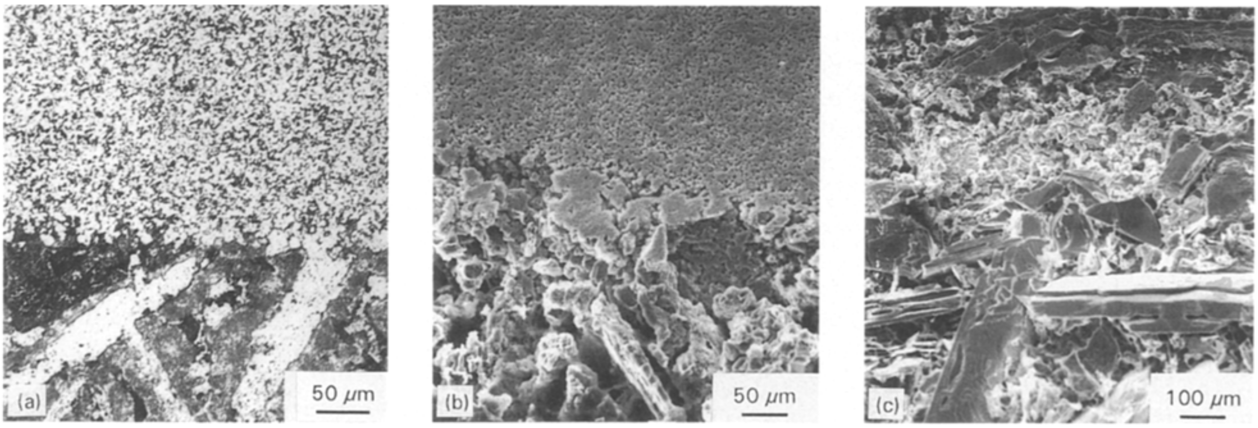

Figure 8 Microstructure of the interface between Al–30Si–1Mg/Si composite and the Al–30Si–1Mg excess alloy. (a) Optical micrograph: upper part Al–30Si–1Mg/Si composite, lower part Al–30Si–1Mg excess alloy. (b) SEM photograph: upper part Al–30Si–1Mg/Si composite, lower part Al–30Si–1Mg excess alloy. (c) SEM photograph of the excess alloy (far away from the interface).

TABLE II Microhardness of Al–Si/Si composites

Alloy	H_V[a]
Al–12Si	68.3(0.5)
Al–30Si	158.6(8.4)
Al–40Si[b]	150(1)
Al–12Si/Si	330(6)
Al–30Si/Si	386(7)

[a] Standard deviation shown in parentheses.
[b] Sumitomo.

TABLE III Compressive strength of Al–Si/Si composites

Alloy	Compressive strength (MPa)[a]
Al–12Si	222.6(7.1)
Al–30Si	377.8(5.4)
Al–12Si/Si	525.7(5.8)
Al–30Si/Si	584.1(13.2)

[a] Standard deviation shown in parentheses.

TABLE IV Tensile strength of Al–Si/Si composites

Alloy	Tensile strength (MPa)[a]
Al–12Si	171.5(5.5)
Al–30Si	65.9(2.5)
Al–40Si[b]	250
Al–12Si/Si	161.1(5.1)
Al–30Si/Si	95.5(3.3)

[a] Standard deviation shown in parentheses
[b] Sumitomo.

TABLE V Scratch width of Al–Si/Si composites

Alloy	Scratch width (mm)[a]
Al–12Si/Si	0.245(0.005)
Al–30Si/Si	0.200(0.010)
Al–40Si[b]	0.315(0.005)

[a] Standard deviation shown in parentheses.
[b] Sumitomo.

of the low strength of Al–30Si, the addition of Si particles to Al–30Si caused strengthening; in contrast, the addition of Si particles to Al–12Si caused slight weakening.

Scratch testing showed that the scratch widths of the Al–12Si–1Mg/Si and Al–30Si–1Mg/Si composites were 0.245 and 0.200 mm, respectively, as compared to a value of 0.315 mm for Sumitomo's Al/Si (40 wt %Si) composite (Table V). The lower scratch width of the composites of this work indicates a greater shear strength.

A composite consisting of interpenetrating networks of two species is attractive for increased thermal conductivity due to the continuity of either species. One species is bound to be more conductive than the other. In our case, aluminium was more conductive than silicon. In general, continuity of the more conductive species is particularly desirable for enhancing the thermal conductivity.

The use of an Al–Si alloy instead of Al as the matrix is known to decrease the CTE of a composite due to the lower CTE of the Al–Si alloy compared to that of Al [8]. However, the use of an Al–Si alloy in conjunction with Si particles as the filler had not been previously reported. Furthermore, the notion of partial dissolution of the filler particles by the liquid alloy for the purpose of forming a filler network had not been previously mentioned. This notion provides a new composite and a new method for composite fabrication. Although the experimental procedure of the method is the same as that of conventional liquid metal infiltration, what happens inside the mould is very different from the case of conventional liquid metal infiltration. The new method is more than just infiltration, as it involves the change of filler particles to a filler network. The network is formed *in situ* during composite fabrication, thus eliminating the need to machine a network into the near-net shape prior to infiltration. The new composite fabrication method is not restricted to Al/Si composites, but it also applies to other eutectic systems such as Ag/Cu, Pb/Sn and Fe/C.

4. Conclusion

New composites comprising interpenetrating networks of silicon (up to 69 vol %) and aluminium (the remaining volume) were fabricated by liquid Al–Si infiltration of a 50 vol % Si particle preform. The dissolution of silicon particles by the Al–Si melt caused a change of silicon from a particulate form to a network form. That the silicon network exceeded 50 vol % of the composite was due to the contribution to the network by the silicon provided by the Al–Si alloy. The network composites were metallurgically sound, with no porosity. The microstructure was uniform with the feature size of the silicon network being about 2–5 μm. The composites had a high compressive strength, high microhardness, high shear strength, low CTE, and low tensile strength compared to commercial Al–Si containing 40 wt %Si.

Acknowledgements

This work was supported by the Advanced Research Projects Agency of the US Department of Defense and the Center for Electronic and Electro-Optic Materials of the State University of New York at Buffalo.

References

1. A. L. GEIGER and M. JACKSON, *Adv. Mater. Process* **7**, (1989) 23.
2. Brochure on CMSH (Sumitomo Electric Industries Ltd, Hyogo, Japan).
3. W. D. CALLISTER Jr, "Materials Science and Engineering", 2nd Edn (Wiley, New York, 1991) p. 662.
4. JENG-MAW CHIOU, *J. Mater. Sci.* **28** (1993) 1471.

5. JINGYU YANG and D. D. L. CHUNG, *ibid.* **24** (1989) 3605.
6. M. K. PREMKUMAR, W. H. HUNT Jr and R. R. SAWTELL, *JOM* **7** (1992) 24.
7. SHY-WEI LAI and D. D. L. CHUNG, *J. Mater. Sci.* in press.
8. N. KUROISHI, Y. ITO, M. KOBAYASHI and M. OSADA, in Proceedings of International Powder Metallurgy Conference and Exhibition Vol. 2., edited by W. A. Kansser and W. J. Happmanm, (Schmid, Freiburg/Br., Germany, 1986) p. 965.

Received 14 April
and accepted 16 May 1994